

The hazard assessment of nanostructured CeO₂-based mixed oxides on the zebrafish *Danio rerio* under environmentally relevant UV-A exposure

Anita Jemec^{a,c*}, Petar Djinović^{a,b}, Ilja Gasan Osojnik Črnivec^a, Albin Pintar^{a,b}

^aNational Institute of Chemistry, Laboratory for Environmental Sciences and Engineering, Hajdrihova 19, SI-1001 Ljubljana, Slovenia

^bCentre of Excellence for Low-Carbon Technologies, Hajdrihova 19, SI-1001 Ljubljana, Slovenia

^cUniversity of Ljubljana, Biotechnical Faculty, Department of Biology, Večna pot 111, SI-1000 Ljubljana, Slovenia

*Corresponding author. Phone: +386 1 3203370; current working address: Biotechnical faculty, University of Ljubljana, Večna pot 111, Ljubljana, Slovenia, e-mail addresses: anita.jemec@bf.uni-lj.si; anita.jemec@gmail.com

Highlights:

- CeO₂-ZrO₂ nanomaterials and pure CeO₂ (up to 100 mg/L) were not harmful to zebrafish
- Only CuO modified CeO₂ affected the growth of zebrafish larvae
- UV-A radiation did not enhance the toxicity of tested nanomaterials

Abstract

The effect of nanomaterials on biota under realistic environmental conditions is an important question. However, there is still a lack of knowledge how different illumination conditions alter the toxicity of some photocatalytic nanomaterials. We investigated how environmentally relevant UV-A exposure (intensity 8.50 ± 0.61 W/m², exposure dose 9.0 J/cm²) affects the toxicity of cerium oxide (CeO₂)-based nanostructured materials to the early-life stages of

zebrafish *Danio rerio*. Pure cerium oxide (CeO₂), copper-cerium (CuO-CeO₂) (with a nominal 10, 15 and 20 mol. % CuO content), cerium-zirconium (CeO₂-ZrO₂) and nickel and cobalt (Ni-Co) deposited over CeO₂-ZrO₂ were tested. It was found that under both illumination regimes none of the tested materials affected the normal development or induced mortality of zebrafish early life stages up to 100 mg/L. Only in the case of CuO-CeO₂, the growth of larvae was decreased (96 h LOEC values for CuCe10, CuCe15 and CuCe20 were 50, 50 and 10 mg/L, respectively). To conclude, CeO₂-based nanostructured materials are not severely toxic to zebrafish and environmentally relevant UV-A exposure does not enhance their toxicity.

Keywords: nickel cobalt nanocrystalline catalysts; UV-A phototoxicity; UV- shielding, zebrafish

1 Introduction

The toxicity of some nanomaterials is altered upon exposure to ultraviolet light, depending on the main constituting components,. Up to now, this has been demonstrated mostly with the TiO₂ nanoparticles, which are the most widely used photocatalysts [Hernández-Alonso et al., 2004]. Elevated phototoxic effects of nano TiO₂ have been reported for plants [Lei et al., 2007], *Gammarus fossarum* [Bundschuh et al., 2011], *Daphnia similis* [Marcone et al., 2012] and zebrafish *Danio rerio* embryos [Bar-Ilan et al., 2012; Clemente et al., 2014; Faria et al., 2014]. There are also reports on the phototoxicity of nano ZnO on nematode *Caenorhabditis elegans* [Ma et al., 2011], and CdSe/ZnSe quantum dots on *Daphnia magna* [Kim et al., 2010]. The major toxic mechanism of phototoxicity is the oxidative stress leading to the potential damage of biomolecules, including DNA, proteins and lipids [Halliwell and Gutteridge, 2007].

Cerium dioxide (CeO₂) nanomaterials have also been suggested as promising photocatalysts [Melchionna and Fornasiero, 2014]. They have broad application in microelectronics, fuel cells, H₂ production/purification, and solid-state electrolytes [Melchionna and Fornasiero, 2014]. CeO₂ has a band gap of 3.2 eV and it is an absorbent for the ultraviolet (UV) radiation, which results in UV-shielding properties that promote their use in the UV-protective sunglass lenses and sunscreen cosmetics [Zholobak et al., 2011]. It has been reported that UV light ($\lambda < 400$ nm) applied on CeO₂ induces a band gap transition,

resulting in the formation of electron-hole pairs. This results in hydroxyl radical and superoxide anion production which may induce oxidative stress [Hernández-Alonso et al., 2004]. CeO₂ nanomaterials are therefore used for water splitting to produce oxygen and degradation of organic contaminants [Bamwenda and Arakawa; 2000; Hernández-Alonso et al., 2004]. On the other hand, CeO₂ has unique electronic structure with oxygen defects, e.g. reactive sites, which can act as free radical scavenging [Zholobak et al., 2011]. Data suggests that nanoceria may reduce cellular structural damage by scavenging the reactive oxygen species: neuronal, ocular, and radioprotection abilities have been demonstrated [reviewed in Hirst et al., 2009].

In this work we assessed the effects of a set of nanostructured materials, such as nanocrystalline CeO₂-based mixed oxides with different optical properties: pure cerium oxide (CeO₂), copper-cerium (CuO-CeO₂) mixed oxide catalysts, cerium-zirconium mixed oxide (CeO₂-ZrO₂) and nickel cobalt bimetallic catalysts (nickel and cobalt deposited over the CeO₂-ZrO₂ nanocrystalline support). The diameters of these nanomaterials range up to several tens of micrometers (primary size), but have nanosized CuO and Ni-Co clusters deposited on the nanocrystalline ceria. According to the latest opinion of the Scientific Committee on Emerging and Newly Identified Health Risks, these nanostructured materials may be referred to as “nanomaterials”, because they encompass “internal structure” in the nano-range (SCENIHR, 2010).

The nanocrystalline CeO₂-based mixed oxides were synthesised in our laboratory for applications in environmental catalysis, such as preferential oxidation of CO in excess H₂ (CO PROX), water-gas shift (WGS) reaction [Djinović et al., 2008], steam reforming of methanol [Udani et al., 2009], catalytic wet-air oxidation (CWAO) of aqueous phenolic solutions [Chen et al., 2007] and CO₂-CH₄ reforming reaction to produce syngas [Djinović et al., 2012, Osojnik Črnivec et al., 2012, 2014]. The advantage of using “in house” NMs is that they are well characterised with known potential impurities and UV-vis diffuse reflectance spectra. Also, all mixed oxides are actually derivatives of the same CeO₂ support. By knowing the exact physicochemical descriptors of these nanomaterials, it will be possible to further use the toxicity data in generation of quantitative nanostructure-activity relationships (QNARs) and read-across approaches (Lynch et al., 2014). Although the production of these nanocrystalline catalysts is at the laboratory scale at the moment, increased testing and future utilization of these materials also present a possibility of their uncontrolled release into the environment.

We have used the early life stages of the *Danio rerio* zebrafish as a test model for the effects of mixed CeO₂-based nanomaterials under different illumination conditions. These

organisms have gained relevance as predictive models for the assessment of the drug-induced toxicity in preclinical studies and are considered as an alternative test system in the environmental risk assessment (<http://www.euroecotox.eu>). Both the embryos and eleutheroembryos (the life interval between the hatch and the onset of exogeneous feeding) are considered alternatives in the context of European legislation [Lammer et al., 2009]. They have become widely used model organisms because of their fecundity, morphological and physiological similarity to mammals, easy and inexpensive maintenance and feasible observation of embryonic development due to their transparency.

The prime goal of this study was to investigate the effects of a set of nanocrystalline CeO₂-based materials with different physicochemical and optical properties on the early life stages of zebrafish. The effects of the materials on the survival and development of zebrafish were investigated under the: (a) visible radiation and (b) simulated environmentally-relevant UV-A radiation.

2 Materials and Methods

2.1 *Synthesis of nanocrystalline CuO-CeO₂ and NiCo/CeO₂-ZrO₂ catalysts*

Pure nanocrystalline CeO₂ and mixed oxide CuO-CeO₂ catalysts with the nominal 10, 15 and 20 mol. % CuO contents (named as CuCe10, CuCe15, and CuCe20, respectively) were synthesized by the hard template method using ordered mesoporous KIT-6 silica [Djinović et al., 2009]. The following chemicals were used as precursors for the synthesis: Cu(NO₃)₂·3H₂O (99.5 % purity, Merck) and Ce(NO₃)₃·6H₂O (99 % purity, Aldrich). Possible impurities resulting from the synthesis were nitrate species originating from Cu(NO₃)₂·3H₂O, ethanol and NaOH (Merck). The NO₃⁻ and ethanol were completely decomposed by heating in an oven [Djinović et al., 2009]. Traces of NaOH were removed by continuously washing samples with deionized water and centrifugation until the pH value reached 7.

The synthesis method produces nanocrystalline CeZr polyhedral materials. The synthesis conditions can be steered in order to decrease the crystallite size and increase their specific surface area and defect chemistry, which is beneficial for their catalytic applications. CeO₂-ZrO₂ mixed oxide (Ce:Zr = 80:20 %, w/w) was synthesised according to the hydrothermal method [Djinović et al., 2012]. The following chemicals were used: cerium (III)

nitrate hexahydrate (Fluka, analytical grade), zirconium (IV) oxynitrate hydrate (Sigma Aldrich, 99 % purity) and NH_4OH (Merck, analytical grade). Traces of NH_4OH were removed by washing several times with deionized water and ethanol, followed by the overnight drying in a laboratory drier at 70 °C and calcination in an oven at 400 °C.

Nickel ($\text{Ni}(\text{NO}_3)_2$) and cobalt ($\text{Co}(\text{NO}_3)_2$) precursors (Merck, analytical grade) were deposited over the $\text{CeO}_2\text{-ZrO}_2$ powdered support at the 40:60 weight ratio using the deposition-precipitation technique [Djinović et al., 2012]. 3, 6, 12 and 18 % (w/w) of Ni-Co loadings were deposited over the support (the materials are named as 3NiCo, 6NiCo, 12NiCo and 18NiCo, respectively). Thermal decomposition of the aqueous urea (Merck, analytical grade) solution was used to initialize the precipitation. The obtained suspension was further washed with deionized water and ethanol to remove the remaining ammonium ions, followed by drying overnight in a laboratory drier at 70 °C. Finally, it was calcined in an oven at 650 °C.

2.2 *Physicochemical characterization of nanomaterials*

Chemical composition of the mixed oxides (w/w % of Cu^{2+}) was determined by inductively-coupled plasma mass spectrometry ([ICP-MS] Agilent Technologies, model 4500 plus, USA). Ni and Co content on $\text{CeO}_2\text{-ZrO}_2$ lattice was determined by inductively-coupled plasma optical emission spectrometry ([ICP-OES] Varian, model 715 ES). Powder X-ray diffraction (XRD) diffractograms of the catalyst samples were recorded on a PANalytical X'pert PRO diffractometer using $\text{CuK}\alpha$ radiation ($\lambda = 0.15406$ nm) [Osojnik Črnivec et al., 2012]. The UV-vis diffuse reflectance spectra of materials were determined with a Perkin Elmer Lambda 35 UV-VIS spectrometer using spectralon as the background.

BET (Brunauer-Emmett-Teller) specific surface area measurements and porosity determination (pore volume) were performed using a Micromeritics ASAP 2020 MP/C apparatus. The apparent particle and agglomerate size was estimated by a field emission scanning electron microscope (FE-SEM, Supra 35 VP, Carl Zeiss, Germany), at an accelerating voltage of 1 kV. The materials were inspected before and after being dispersed in the toxicity test media.

The size of nanomaterials in ISO medium (ISO 15088:2007) were inspected using the dynamic light scattering technique (Microtrac S3500, UK).

2.3 *Preparation of the nanomaterial dispersions*

The nanomaterials were dispersed in the ISO medium (ISO 15088:2007). The solutions were always prepared freshly prior to the experiment. The suspensions were sonicated for 15 min using a probe sonicator (Hielscher, model UP200S) at 50 % amplitude and 0.5 cycle duration. The concentrations tested were 1, 10, 50 and 100 mg/L of nanomaterials. The exposure concentrations were selected based on previous experiments published in Jemec et al. (2012), where 100 mg/L was found non-lethal and did not induce zebrafish malformations under room light. This enabled us to follow the expected potential increase in toxicity caused by UV-A. Another reason for choosing 100 mg/L is because this is a threshold in aquatic toxicity studies, above which the chemical is no longer considered toxic (EEC Directive 93/67).

2.4 *Toxicity to the early life stages of the zebrafish *Danio rerio**

Two exposure conditions were employed in the toxicity tests: (2.4.1.) visible radiation and (2.4.2) simulated environmentally-relevant UV-A radiation. Experiments under the visible radiation were performed only with the CeO₂-ZrO₂- based nanomaterials, because pure CeO₂ and CuCe mixed oxides have been published previously [Jemec et al., 2012] and are discussed here only for the comparison. UV-A exposure experiments with all the nanomaterials are presented in this paper.

Toxicity tests and zebrafish eggs breeding were performed according to Jemec et al. [Jemec et al., 2012]. The procedure is in principle a modified protocol of ISO 15088:2007, since the exposure was prolonged up to 4 days. Larvae were not fed during the test, as it is suggested in the OECD 212 procedure [OECD 212]. Adult zebrafish were bred in a temperature-controlled room in aquarium (60 × 30 × 30 cm) containing 45 L of tap water with constant temperature (26 °C) and controlled photoperiod conditions (12 h light : 12 h dark). On the day before breeding, a plastic spawning box covered with stainless steel mesh was placed in the breeding tank. On the following day, one hour after the light cycle started, the spawning plastic box was removed from the tank and eggs were collected.

2.4.1 Visible radiation

In the visible radiation exposure regime, individual eggs of age 3 hpf (3 hours post fertilization) were placed into the test containers (24-hole microwell plate), each in 1 mL of test media. In the each test, 10 eggs per control containing only ISO medium (ISO 15088:2007) and 10 eggs per each concentration of the nanomaterial suspension were exposed. Concentrations up to 100 mg/L were tested. Four independent experiments were done (performed at different times with freshly prepared test medium each time) for each of the nanomaterials. Forty eggs were exposed per each test concentration of each nanomaterial altogether.

The test plate was covered with a transparent plastic self-adhesive foil to prevent the evaporation of the medium. Malformations of the embryos were evaluated after 24 and 48 h of exposure [Tišler et al., 2009]. Every day onwards after the embryos hatched (up to 4 days post fertilization), the larvae were inspected for the mortality, developmental malformations and growth (body length) using a stereoscopic microscope (Nikon SMZ 1000 equipped with a DS-Fi1 digital camera) and a NIS-Elements Documentation 2.2 imaging software. Lethal malformations (i.e. egg coagulation, missing heartbeat, missing somites, missing tail detachment from the yolk sac) and non-lethal malformations (i.e. no eye and body pigmentation, missing blood flow, spine deformation, yolk sac edema, incomplete eye and ear development) were evaluated.

Along with a negative control containing only the ISO medium (ISO 15088:2007), also a positive control with the reference chemical, 3,4-dichloroaniline, was always prepared to check for the sensitivity of the embryos. The concentrations tested were 2, 2.5, 3 and 3.7 mg/L. The sensitivity of the embryos between the experiments did not differ, since the 24 h and 48 h LC₅₀ (based on at least one of the lethal malformations) were always within the narrow ranges: 2.2-3.0 mg/L and 2.3-2.6 mg/L, respectively.

Visible radiation was provided by Osram cool white lamp (L 58W/640). No UV-A or UV-B was detected under visible radiation (UVX radiometer, UVP).

2.4.2 Simulated environmentally-relevant UV-A radiation

Emission spectrum of the UV-A lamp with the peak intensity at 365 nm is shown in **Fig. 1**. Mean intensity of the radiation under the UV-A lamp was $8.50 \pm 0.61 \text{ W/m}^2$. We calculated

UV-A exposure doses as the intensity of the radiation (W/m^2) multiplied by the duration of the exposure(s), gaining exposure doses in J/cm^2 .

In the UV-A experiments, zebrafish were individually placed into 1 mL of test medium in borosilicate glass dishes, each 1 cm in diameter. These were placed into an aluminium holder which was placed under the UV-A light for a defined exposure duration (depending on the radiation dose of the UV-A applied). Glass dishes instead of plastic ones were used to prevent possible effects of the UV- induced plastic degradation products on zebrafish. The whole holder was covered with a transparent plastic self-adhesive foil to prevent the evaporation of the medium (**SI Fig. S1 Supplementary data**). We checked that the transparent foil did not decrease the intensity of UV-A radiation. Constant temperature ($26\text{ }^\circ\text{C}$) was maintained during the UV-A exposure. After the exposure to UV-A light, the embryos were transferred to the same experimental conditions as were applied in the visible radiation experiments. The tests were performed in the same manner as in the visible radiation regime; 10 eggs per each concentration of the nanomaterial suspensions were exposed and the test was repeated four times. The same parameters (mortality, malformations and body length) were inspected.

Prior to the toxicity experiments with the nanomaterials, the toxicity of UV-A for the zebrafish embryos and larvae was determined. The following exposure doses were applied: 9.0, 15.3, 24.48, 36, 55 and $73.44\text{ J}/\text{cm}^2$ (the mean intensity was always the same, e.g. $8.50 \pm 0.61\text{ W}/\text{m}^2$, but the duration of exposure varied). Experiments were performed with fertilized eggs of two developmental stages, i.e. 2 hpf (hours post fertilization) and 3 hpf. Based on the findings of these preliminary experiments, we used embryos of age 3 hpf and exposure dose of $9.0\text{ J}/\text{cm}^2$ in phototoxicity experiments with the nanomaterials. This exposure enabled undisturbed development of larvae due to the UV-A exposure and the effects of the nanomaterials could be observed.

2.4.3 *UV-A shielding properties of the CeO_2 -based nanostructured mixed oxides*

Because CeO_2 was previously reported to have UV-shielding properties, we also investigated if CeO_2 -based nanostructured mixed oxides could act as UV-A filters. Only those materials which exhibited no effect on the larvae (CeO_2 , $\text{CeO}_2\text{-ZrO}_2$ and 18 NiCo) were used in this experiment in order to follow only the effect of the UV-A and not the materials themselves. In these experiments, such a high UV-A exposure dose was used that the normal development of the larvae was affected ($36.7\text{ J}/\text{cm}^2$ (12 h of exposure)); embryos of age 3 hpf

were used). We checked if the presence of CeO₂, CeO₂-ZrO₂ and 18 NiCo materials (all at the 100 mg/L concentration) prevented abnormal development of larvae. Experimental set-up was the same as described in the section 2.4.2 (Simulated environmentally-relevant UV-A radiation).

2.5 Data analysis

Results are presented as the share of abnormal larvae (dead and deformed) observed after 4 days. The body length was measured as the distance from the most anterior part of the head to the tip of the tail, following the path of the developing spinal cord. Larvae with spine deformities were not inspected for length.

One-way Analysis Of Variance (ANOVA) with the Mann-Whitney post-hoc test was used to test the differences between the control and different concentrations of the nanomaterials. The data were normally distributed and the variance was homogenous as determined in the Levene's test. Lowest-observed effect concentration (LOEC) was determined as the lowest concentration producing statistically significant response ($p < 0.05$). All tests were done using Statgraphics software (Statgraphics Plus for Windows 4.0, Statistical Graphics Corporation).

3 Results

3.1 Physico-chemical properties of the nanomaterials

Physico-chemical properties of the nanomaterials are depicted in SI **Table S1 (Supplementary data)**. In general, CeO₂-ZrO₂-based materials exhibited significantly lower BET specific surface area than the CeO₂-based nanomaterials, which originates from the hard template synthesis method used for their preparation. Pure CeO₂ exhibited lower BET specific surface area than the CuO-CeO₂ oxides; among these, CuCe10 catalyst had lower surface area in comparison to the CuCe15 and CuCe20 solids. Concerning CeO₂-ZrO₂ materials, CeO₂-ZrO₂ exhibited higher BET specific surface area than NiCo bimetallic catalysts. It is further evident from the SI Table S1 (Supplementary data) that CuO clusters deposited on the

nanocrystalline ceria are an order of magnitude smaller in comparison to the NiCo clusters deposited on the surface of the CeO₂-ZrO₂ support prepared by hydrothermal synthesis.

The nanostructure of the investigated nanomaterials is evident from the clearly defined crystalline planes, as resolved in the HR-TEM images. Small NiCo clusters (about 6 nm) are dispersed over the CeZr nanoparticles deposited onto CeO₂ (which are about 10-15 nm in size, according to the attached TEM images) (**SI Fig. S2, Supplementary data**).

SEM micrographs revealed that particles of all the materials are very irregularly shaped and polydisperse in diameters up to several tens of micrometers. In this respect, no differences between the nanomaterials could be found. Also, SEM showed no change in the size of particles after being dispersed in the toxicity test media (**SI Fig. S3, Supplementary data**).

The median sizes of the CeO₂ and CuCe nanomaterials in the ISO medium (ISO 15088:2007) obtained by dynamic light scattering analysis were previously reported by Jemec et al. [2012]. In summary, median sizes of these materials were in the range of 9.15-9.95 μm and no difference between the materials was found. The size of nanomaterials was independent on the nanomaterial concentration and was unchanged during the course of the experiments.

Copper loading on materials was measured by ICP-MS. The following shares of Cu were determined: 3.5, 5.3 and 7.2 % (w/w) at CuCe10, CuCe15 and CuCe20 samples, respectively. The concentrations of Ni and Co on the nanomaterials were within 90 % of the nominal loadings, and the ratio between Ni and Co (40:60) was unchanged.

To investigate the optical properties of the studied materials, UV-vis diffuse reflectance was measured and the results are presented in **Fig. 1**. A clear difference between the materials was found. The absorption spectra of pure CeO₂ and CeO₂-ZrO₂ mixed oxide can be assigned to the intrinsic transition from the valence band to the conduction band [Wang et al., 2014] and exhibit an evident absorption decrease in the range of 350 to 450 nm. In the case of CuO-CeO₂ mixed oxides, the absorption edge extends a red shift to the visible spectrum (400 to 700 nm), which is due to the presence of lower bandgap semiconductors [Saravanan et al., 2013]. Therefore, in emission peak range of UV-A lamp (300-400 nm) CeO₂-ZrO₂ sample had the lowest absorbance, followed by NiCo materials, pure CeO₂ and finally CuO-CeO₂ mixed oxides, which exhibited the highest capability for the absorption of the UV-A light.

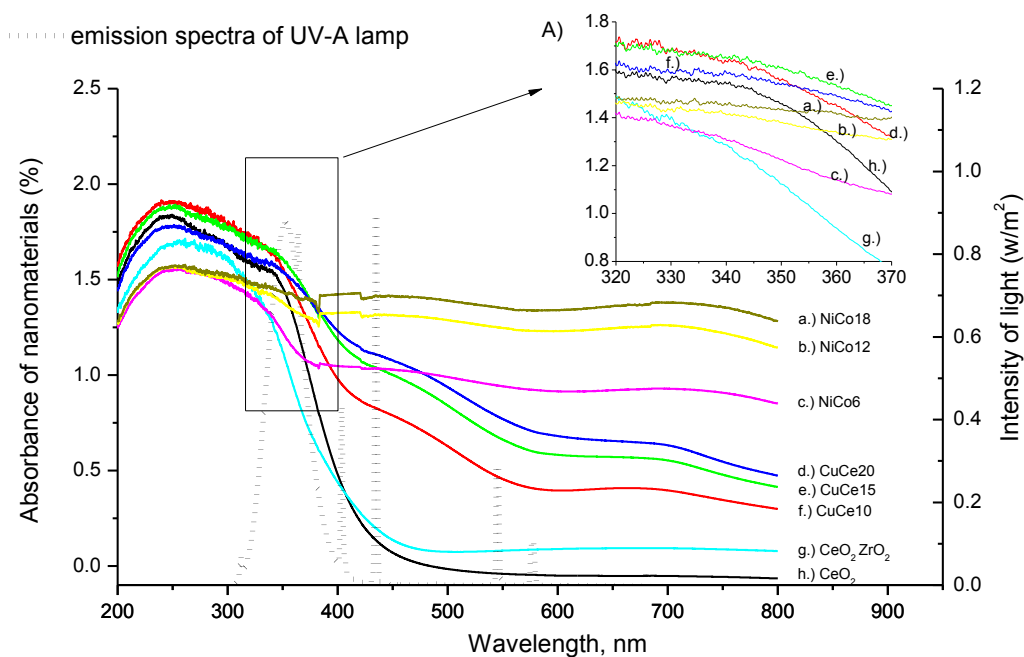


Fig. 1. Emission spectra of the UV-A lamp and UV-vis diffuse reflectance spectra of the nanomaterials. (A) the range between 320-370 nm is magnified (a-h refer to the name of nanomaterials explained in the main diagram). (Please refer to colour photo published online for better clearance.)

3.2 Effects of the UV-A on the zebrafish *Danio rerio*

Prior to the toxicity experiments with the nanomaterials, the toxicity of UV-A for the zebrafish embryos and larvae was determined. The survival of the zebrafish under the UV-A exposure depends greatly on the age of the embryos at the time of the exposure (**Fig. 2a**). Those of the age 2 hpf were more sensitive to the UV-A exposure. NOEC for both ages of the embryos was set at 9.0 J/cm^2 . LD₅₀ values were established at 18 J/cm^2 for the 2 hpf and 29 J/cm^2 for the 3 hpf embryos. Therefore, in all the subsequent phototoxicity experiments with the nanomaterials, 3 hpf embryos were used and exposure dose of 9.0 J/cm^2 was applied to ensure the undisturbed development of the control group of larvae. In this way, we were able to evaluate joint effects of the nanomaterials and UV-A.

Length of larvae after 4 days was also measured. In the case of the 3 hpf embryos, length was unaffected up to 24.5 J/cm^2 , while the 2 hpf embryos had decreased length at this dose (**Fig. 2b**).

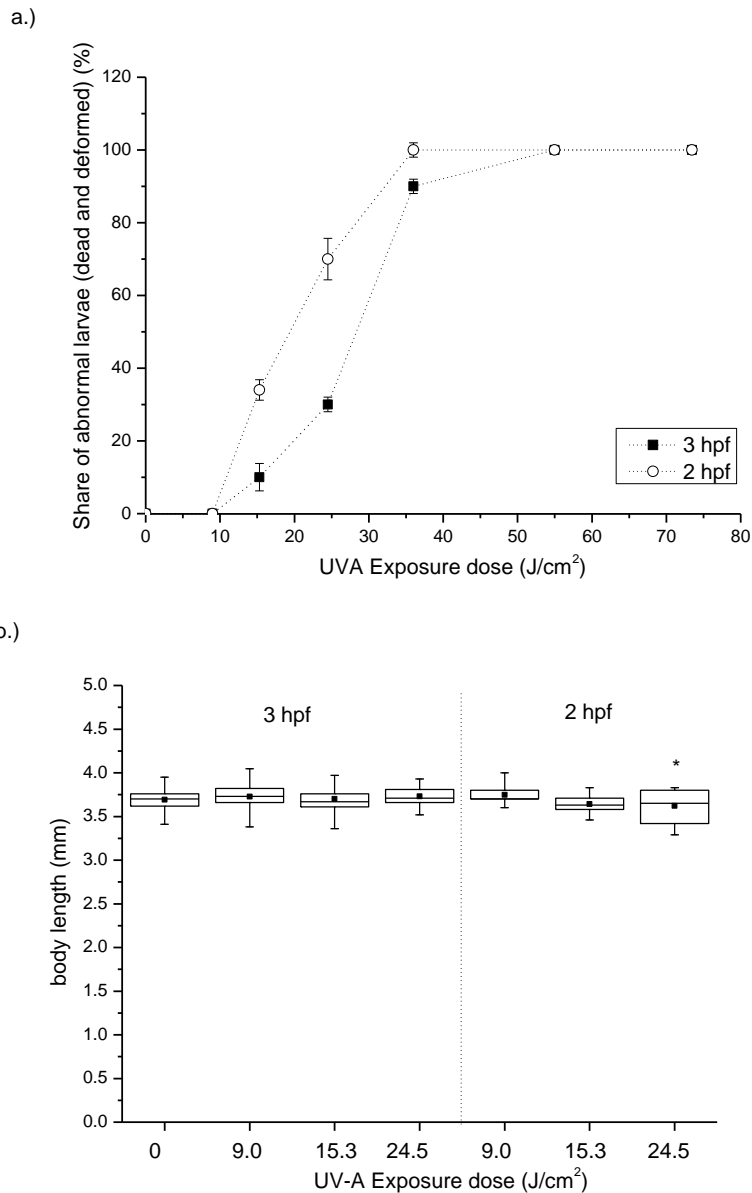


Fig. 2. Development of the zebrafish larvae (a) and body length (b) 4 days after exposure to the UV-A. Embryos of age 2 hpf (hours post fertilization) and 3 hpf were exposed. Please note that the 2 hpf embryos are more sensitive to the UV-A than the 3 hpf. Symbols on the box plot represent: maximum and minimum value (whiskers: \perp), mean value (\blacksquare), outliers (-), and statistically significant difference in comparison to the control ($p < 0.05$, *).

3.3 Effects of the nanomaterials on the zebrafish *Danio rerio*

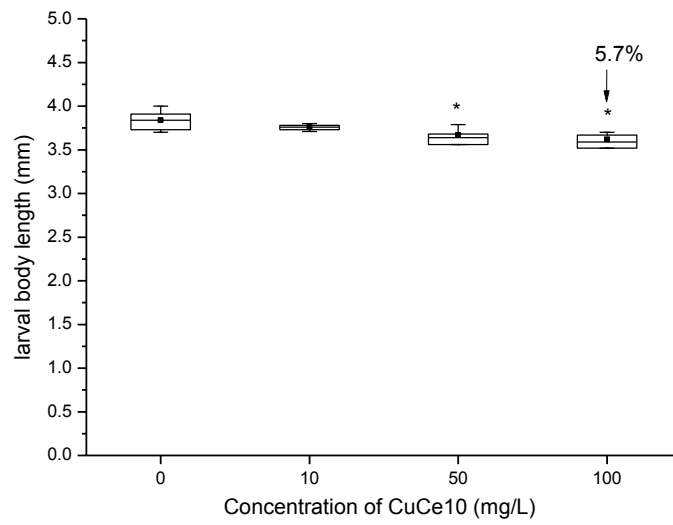
3.3.1 Visible radiation

CeO₂-ZrO₂, 3NiCo, 6NiCo, 12NiCo and 18NiCo materials had no effects on the mortality, occurrence of developmental malformations or growth (body length) of the zebrafish up to 100 mg/L (**Fig. S4, Suppl. data**). Testing of pure CeO₂ and CuCe mixed oxides under visible light was done in a previous study (Jemec et al, 2012): 4d LOEC_{body length} for CuCe10, CuCe15 and CuCe20 solids were 50, 50 and 10 mg/L, respectively. No effect of pure CeO₂ was found up to 100 mg/L (data are given for comparison to the UV-A exposure).

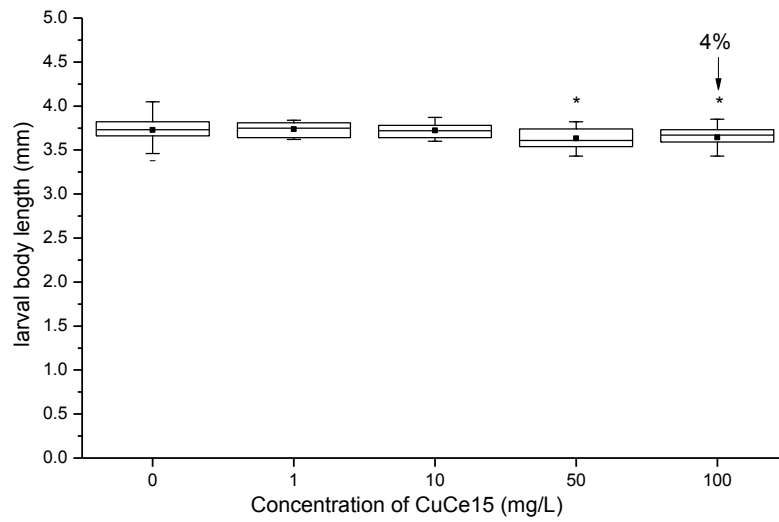
3.3.2 UV-A radiation

Under the UV-A exposure conditions (9.0 J/cm²), no effects of pure CeO₂, CeO₂-ZrO₂, 3NiCo, 6NiCo, 12NiCo and 18NiCo samples on the zebrafish were found up to 100 mg/L. For CuCe mixed oxides, no developmental malformations (were observed up to 100 mg/L, but the body length was affected. The 4 d LOEC_{body length} were: 50, 50 and 10 mg/L for CuCe10, CuCe15 and CuCe20 solids, respectively (**Fig. 3 a-c**).

a.)



b.)



c.)

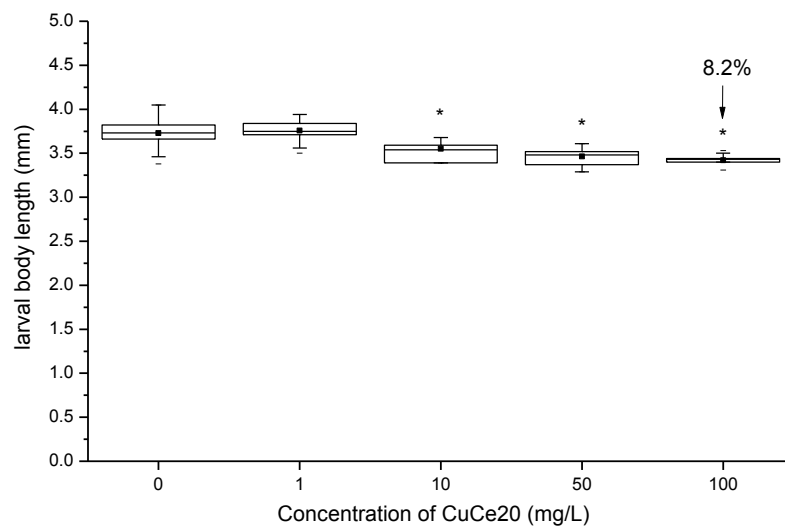


Fig. 3. Larval body length after 4 days of the exposure to CuCe10 (a), CuCe15 (b) and CuCe20 (c) samples under the UV-A irradiation. The percentage of growth retardation in comparison to the control is noted. Symbols on the box plot represent: maximum and minimum value (whiskers: \perp), mean value (\blacksquare), outliers (-), and $p < 0.05$ (*). 3 hpf larvae and a radiation dosage of 9.0 J/cm^2 were used.

3.4 UV-A shielding properties of CeO_2 -based nanomaterials

In the UV-shielding experiments (applied UV-A radiation dose 36.7 J/cm^2), 90 % of control larvae were deformed. However, all the tested nanomaterials, CeO_2 , $\text{CeO}_2\text{-ZrO}_2$ and 18NiCo samples (all at the 100 mg/L concentration), significantly prevented abnormal development of the larvae (0, 5 and 10 % abnormal larvae were observed, respectively) (**Fig. 4**).

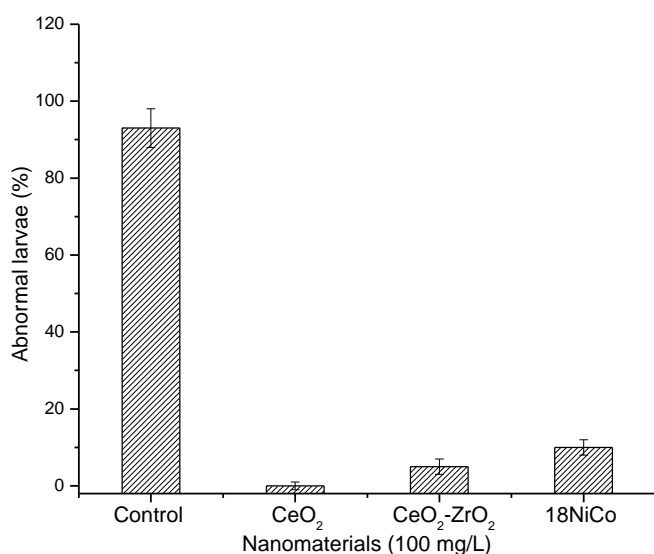


Fig. 4. The UV-A shielding effect of the nanomaterials (100 mg/L). The share of abnormal larvae (dead and deformed) is significantly decreased in the presence of the nanomaterials (standard deviation is shown). 3 hpf larvae and a radiation dosage of 36.7 J/cm^2 were used. Please note, that all tested nanomaterials significantly prevent UV-A damage to zebrafish.

4 Discussion

We studied the effects of the nanocrystalline CeO₂-based materials with different physico-chemical and optical properties on the early-life stages of the zebrafish *Danio rerio* under two illumination conditions: visible radiation and environmentally-relevant UV-A radiation. In the emission peak range of the UV-A lamp, the CeO₂-ZrO₂ sample had the lowest absorbance, followed by the NiCo materials and pure CeO₂, and CuCe mixed oxides, which exhibited the highest absorbance. If we compare the results for the CeO₂, CeO₂-ZrO₂, 3NiCo, 6NiCo, 12NiCo and 18NiCo samples toxicity under the UV-A and visible light (data for pure CeO₂ and CuCe mixed oxides are taken from Jemec et al., 2012], no differences in the effects of these materials on the zebrafish can be found regardless of the different UV-vis diffuse reflectance spectra. We therefore conclude that CeO₂ nanomaterials investigated in this work do not induce UV-A-related phototoxic effects.

In the experiments with high UV-A radiation dose (36.7 J/cm²), 100 mg/L of CeO₂, CeO₂-ZrO₂ and 18NiCo solids significantly decreased the effects of the UV-A light (from 90%, as observed in control, to 0%). This concentration of the nanomaterials was tested because it was previously established as a 4 d NOEC (Jemec et al., 2012). However, because of the high concentration of solids, the UV-A shielding is most probably due to their absorption onto the chorion, thus preventing the physical access of the UV-A to the embryos. To confirm the genuine UV-A shielding effects of the CeO₂-based nanomaterials (absorption of the UV-A and antioxidant activity), as suggested by the literature data [Hirst et al., 2009; Zholobak et al., 2011], we suggest that further systematic studies with lower concentrations of the nanomaterials should be performed. This refers also to the other types of photocatalytic materials.

All the CeO₂-ZrO₂-based catalysts and pure CeO₂ proved to be completely non-harmful to the zebrafish up to 100 mg/L, but mixed CuCe oxides affected the growth of the larvae (4d LOEC values for CuCe10, CuCe15 and CuCe20 solids were 50, 50 and 10 mg/L, respectively). We could not explain the observed differences in the toxicity with primary physico-chemical properties of the tested nanomaterials, such as BET specific surface area, size of aggregates in the test medium and chemical composition of nanomaterials (as described in **Table S1**). This is in line with the most recent advancements in this field, where it has become clear that primary physico-chemical descriptors of nanomaterials are not the most appropriate to predict their toxicological potential (Lynch et al., 2014). The reason is that nanomaterials change in biological media (i.e. are affected by the surrounding matrix,

pH, ionic strength, biomolecules, etc.) and gain their secondary “extrinsic” properties. Many nanomaterials’ properties are inter-dependent, meaning that change in one property (for example shape) may influence another property (e.g. surface chemistry). The “secondary derived feature of nanomaterials”, such as the release of metals (Lynch et al., 2014), is another aspect of this phenomenon. In this context, we have previously ruled out that dissolved Cu may be the reason for the observed toxicity in the case of CuCe materials. The share of dissolved Cu^{2+} from the CuCe materials is very small and does not explain the observed toxicity [Jemec et al., 2012].

It is only recently that zebrafish embryos have been applied in the photo-induced nanotoxicity studies [Bar-Ilan et al., 2012; Clemente et al., 2014; Faria et al., 2014]. We have reviewed the data on the experimental conditions used by different authors (**Table S2, Suppl. data**). Very different illumination intensities, durations of exposure, and age of embryos at the time of exposure (from 1 hour post fertilization up to 7 days post fertilization) were applied. This makes the comparison of the results very difficult. Consequently, the effect values for the survival of the control fish were very variable. Some of the authors exposed the fish to nano TiO_2 under UV exposure, which already caused harmful effects on the control fish [Clemente et al., 2014; Faria et al., 2014]. However, no interaction between the concurrent effect of the UV and TiO_2 has been taken into consideration. Most of the authors exposed the fish in plastic multi-well plates, but we rather suggest glass dishes to prevent the interaction between the UV and plastic. Clearly, the illumination experimental set-ups in photo-induced nanotoxicity studies will have to be standardised. Significantly more effort should be put into the development of relevant and realistic illumination conditions. We exposed the fish to the UV-A radiation ($8.50 \pm 0.61 \text{ W/m}^2$) that is close to the ambient values (mean summer peak daily irradiances at clear skies in different cities across the world were found in the range of $33.99\text{-}64.26 \text{ W/m}^2$, while mean winter values were in the range of $0.72\text{-}37.73 \text{ W/m}^2$) [Häder et al., 2007]. However, unrealistic intensities have been applied in some studies (7050 W/m^2) [Dong et al., 2007].

In conclusion, all the $\text{CeO}_2\text{-ZrO}_2$ -based catalysts and pure CeO_2 proved to be completely non-hazardous to the zebrafish embryos both under the visible light and the UV-A radiation. Only copper-doped CeO_2 showed some sublethal effects on the growth of larvae. The CeO_2 -based nanomaterials do not exhibit UV-A-related phototoxic effects to the zebrafish at the given radiation dose. The currently established classification system in aquatic toxicity testing relies on ranking according to the EC50 values: $<0.1 \text{ mg/L}$ =extremely toxic; $0.1\text{-}1 \text{ mg/L}$ = very toxic; $1\text{-}10 \text{ mg/L}$ = toxic; $10\text{-}100 \text{ mg/L}$ = harmful; $<100 \text{ mg/L}$ = non-toxic to the aquatic

organisms (EEC Directive 93/67). In this study, the EC50 could not be determined due to the lack of such high response. The results of this study therefore suggest that no severe hazard of these nanomaterials for the environment exists and from this perspective further development of such environmental catalysts is encouraged.

Acknowledgements

The authors gratefully acknowledge the financial support of the Ministry of Education, Science and Sport of the Republic of Slovenia through the Research program P2-0150. This work was financially supported by the Slovenian Research Agency project number Z1-2107. We thank Tea Romih for English language editing.

Appendix A. Supplementary data

Supplementary data associated with this article can be found in the online version

References

- Bamwenda G.R., H. Arakawa. Cerium dioxide as a photocatalyst for water decomposition to O_2 in the presence of $Ce(aq)^{4+}$ and $Fe(aq)^{3+}$ species. *J. Mol. Catal. A-Chem* 161 (2000) 105-113.
- Bar-Ilan O., K.M. Louis, S.P. Yang, J.A. Pedersen, R.J. Hamers, R.E. Peterson, W. Heideman, Titanium dioxide nanoparticles produce phototoxicity in the developing zebrafish, *Nanotoxicology* 6 (2012) 670-9.
- Bundschuh M., J.P. Zubrod, D. Englert, F. Seitz, R.R. Rosenfeldt, R. Schulz, Effects of nano- TiO_2 in combination with ambient UV-irradiation on a leaf shredding amphipod, *Chemosphere* 85 (2011) 1563-7.
- Chen, I.P., S.S. Lin, C.H. Wang, S.H. Chang, CWAO of phenol using $CeO_2/\gamma-Al_2O_3$ with promoter—Effectiveness of promoter addition and catalyst regeneration, *Chemosphere* 66 (2007) 172-178.
- Clemente Z., V.L. Castro, M.A. Moura, C.M. Jonsson, L.F. Fraceto, Toxicity assessment of TiO_2 nanoparticles in zebrafish embryos under different exposure conditions, *Aquat. Toxicol.* 147 (2014) 129-39.
- Djinović P., U. Kocjan, J. Batista, A. Pintar, Synthesis and Characterization of Ordered $CuO-CeO_2$ Mixed Oxides Using KIT-6 Silica as a Hard Template, *Acta. Chim. Slov.* 56 (2009) 868-877.

- Djinović, P., I.G. Osojnik Črnivec, B. Erjavec, A. Pintar, Influence of active metal loading and oxygen mobility on coke-free dry reforming of Ni–Co bimetallic catalysts, *Appl. Catal. B* 125 (2012) 259-270.
- Djinović P., J. Levec, A. Pintar, Effect of structural and acidity/basicity changes of CuO–CeO₂ catalysts on their activity for water–gas shift reaction, *Catal. Today* 138 (2008) 222–227.
- Dong Q., K. Svoboda, T.R. Tiersch, W.T. Monroe, Photobiological effects of UVA and UVB light in zebrafish embryos: evidence for a competent photorepair system, *J. Photochem. Photobiol. B.* 88 (2007) 137-46.
- EEC Directive 93/67. Commission of the European Communities, 1996. Technical guidance document in support of commission directive 93/67/EEC on risk assessment for new notified substances and commission regulation (EC) No.1488/94 on risk assessment for existing substances. Part II: Environmental Risk Assessment. Luxembourg.
- Faria M., J.M. Navas, A.M. Soares, C. Barata, Oxidative stress effects of titanium dioxide nanoparticle aggregates in zebrafish embryos, *Sci. Total. Environ.* 470-471 (2014) 379-89.
- Häder D.P., M. Lebert, M. Schuster, L. del Ciampo, E.W. Helbling, R. McKenzie, ELDONET-a decade of monitoring solar radiation on five continents, *Photochem. Photobiol.* 83 (2007) 1348-57.
- Halliwell B., J.M.C. Gutteridge, 2007. *Free Radicals in Biology and Medicine*. Oxford University Press, New York, USA.
- Hernandez-Alonso M., A.B. Hungria, A. Martinez-Arias, M. Fernandez-Garcia, J.M., Coronado, J.C. Conesa, J. Soria. EPR study of the photoassisted formation of radicals on CeO₂ nanoparticles employed for toluene photooxidation. *Applied catalysis B-environmental* 50 (2004) 167-175.
- Hirst S.M., A.S. Karakoti, R.D. Tyler, N. Sriranganathan, S. Seal, C.M. Reilly. Anti-inflammatory properties of cerium oxide nanoparticles. *Small.* 5 (2009) 2848-56.
- ISO 15088. Water quality-Determination of the acute toxicity of waste water to zebrafish eggs (*Danio rerio*), International Standardisation Organisation, Geneva, Switzerland. (2007).
- Jemec A., P. Djinović, T. Tišler, A. Pintar, Effects of four CeO₂ nanocrystalline catalysts on early-life stages of zebrafish *Danio rerio* and crustacean *Daphnia magna*, *J. Hazard. Mater.* 219-220 (2012) 213-20.
- Kim J.,Y. Park, T.H. Yoon, C.S., K. Choi, Phototoxicity of CdSe/ZnSe quantum dots with surface coatings of 3-mercaptopropionic acid or tri-n-octylphosphine oxide/gum arabic in

- Daphnia magna* under environmentally relevant UV-B light, *Aquat. Toxicol.* 97 (2010) 116-24.
- Lammer E., G.J. Carr, K. Wendler, J.M. Rawlings, S.E. Belanger, T. Braunbeck, Is the fish embryo toxicity test (FET) with the zebrafish (*Danio rerio*) a potential alternative for the fish acute toxicity test? *Comp. Biochem. Physiol. C Toxicol. Pharmacol.* 149 (2009) 196-209.
- Lei Z., S. Mingyu S, L. Chao, C. Liang, H. Hao, W. Xiao, L. Xiaoqing, Y. Fan, G. Fengqing, H. Fashui. Effects of Nanoanatase TiO₂ on photosynthesis of spinach chloroplasts under different light illumination, *Biol. Trace. Elem. Res.* 119 (2007) 68-76.
- Lynch I., Weiss C., Valsami-Jones, E. A strategy for grouping of nanomaterials based on key physico-chemical descriptors as a basis for safer-by-design NMs. *Nano Today* 9 (2014) 266-270.
- Ma H., N.J. Kabengi, P.M. Bertsch, J.M. Unrine, T.C. Glenn, P.L. Williams, Comparative phototoxicity of nanoparticulate and bulk ZnO to a free-living nematode *Caenorhabditis elegans*: the importance of illumination mode and primary particle size. *Environ. Pollut.* 159 (2011) 1473-80.
- Ma H., S.A. Diamond, Phototoxicity of TiO₂ nanoparticles to zebrafish (*Danio rerio*) is dependent on life stage, *Environ. Toxicol. Chem.* 32 (2013) 2139-43.
- Marcone G.P., A.C. Oliveira, G. Almeida, G.A. Umbuzeiro, W.F. Jardim, Ecotoxicity of TiO₂ to *Daphnia similis* under irradiation, *J. Hazard. Mater.* 211-212 (2012) 436-42.
- Melchionna M., P. Fornasiero. The role of ceria-based nanostructured materials in energy applications. *Materials Today* (2014), In Press, Corrected Proof
- OECD 212. Guidelines for the Testing of Chemicals. Fish, Short-term Toxicity Test on Embryo and Sac-fry Stages, (1998).
- Osojnik Črnivec, I. G., A. Pintar, Toward enhanced conversion of model biogas mixtures: Parametric tuning and mechanistic study for ceria-zirconia supported nickel-cobalt catalyst, *Catal Sci Technol* (2014), in press, doi:10.1039/C3CY01079A
- Osojnik Črnivec, I.G., P. Djinović, B. Erjavec, A. Pintar, Effect of synthesis parameters on morphology and activity of bimetallic catalysts in CO₂-CH₄ reforming, *Chem. Eng. J* 207-208 (2012) 299-307.
- Saravanan R., S. Joicy, V.K. Gupta, V. Narayanan, A. Stephen, Visible light induced degradation of methylene blue using CeO₂/V₂O₅ and CeO₂/CuO catalysts, *Mater. Sci. Eng. C* 33 (2013) 4725-4731.

- SCENIHR (Scientific Committee on Emerging and Newly Identified Health Risks), Opinion on the scientific basis for the definition of the term “nanomaterial”, 8 December 2010.
- Tišler T., A. Jemec, B. Mozetič, P. Trebše, Hazard identification of imidacloprid to aquatic environment, *Chemosphere* 76 (2009) 907-914.
- Udani, P.P.C.; P.V.D.S Gunawardana, H.C. Lee, D. H. Kim, Steam reforming and oxidative steam reforming of methanol over CuO–CeO₂ catalysts, *Int. J. Hydrogen Energ.* 34 (2009) 7648-7655.
- Van Hoecke K., J.T. Quik, J. Mankiewicz-Boczek, K.A. De Schampheleere, A. Elsaesser, P. Van der Meeren, C. Barnes, G. McKerr, C.V. Howard, D. Van de Meent, K. Rydzyński, K.A. Dawson, A. Salvati, A. Lesniak, I. Lynch, G. Silversmit, B. De Samber, L. Vincze, C.R. Janssen, Fate and effects of CeO₂ nanoparticles in aquatic ecotoxicity tests, *Environ. Sci. Technol.* 43 (2009) 4537-4546.
- Wang Y., F. Wang, Y. Chen, D. Zhang, B. Li, S. Kang, X. Li, L. Cui, Enhanced photocatalytic performance of ordered mesoporous Fe-doped CeO₂ catalysts for the reduction of CO₂ with H₂O under simulated solar irradiation. *Appl. Catal. B Environmental* 147 (2014) 602-609.
- Zholobak N.M., V.K. Ivanov, A.B. Shcherbakov, A.S. Shaporev, O.S. Polezhaeva, A.Y. Baranchikov, N.Y. Spivak, Y.D. Tretyakov, UV-shielding property, photocatalytic activity and photocytotoxicity of ceria colloid solutions, *J Photochem. Photobiol. B.* 102 (2011) 32-8.